Challenge Journal of CONCRETE RESEARCH LETTERS

Research Article

Effect of polyethylene terephthalate granules on nano-$CaCO_3$-blended concrete

Awinash Kumar [a], Sachin Kumar Singh [a], Abhishek Mishra [a], Awadhesh Srivastava [a,*]

[a] *Department of Civil Engineering, Institute of Engineering and Technology, Lucknow, 226021 Uttar Pradesh, India*

ABSTRACT

This study explores the effects of partially replacing fine aggregate with 10% polyethylene terephthalate granules (PET) and cement with varying amounts (0–5%) of nano calcium carbonate ($CaCO_3$) in M40 grade concrete. Concrete mixes were tested for workability, density, compressive strength, tensile strength, and flexural strength. Microstructural characteristics were examined using Scanning Electron Microscopy (SEM) and X-Ray Diffraction (XRD), while ANSYS simulations were used to validate compressive strength results. The results indicated that the optimal performance was achieved at 2% nano-$CaCO_3$ replacement along with 10% PET. Although workability and density slightly declined with increasing $CaCO_3$ content, compressive and tensile strengths showed only minor reductions, reflecting the limited reactivity of $CaCO_3$. On the other hand, the addition of PET improved flexural strength and toughness, though these benefits reduced gradually at higher $CaCO_3$ levels. SEM and XRD analyses confirmed uniform dispersion and the presence of crystalline phases, while ANSYS simulations closely matched experimental results, reinforcing the validity of the findings. The study is limited to M40 grade concrete and specific replacement levels. However, the findings suggest that combining PET waste and nano-$CaCO_3$ can enhance mechanical performance while contributing to environmental benefits by reducing plastic waste and CO_2 emissions. Further research is needed for broader application and lifecycle assessment.

ARTICLE INFO

Article history:
Received – June 25, 2025
Revision requested – September 1, 2025
Revision received – September 4, 2025
Accepted – September 15, 2025

Keywords:
Polyethylene terephthalate
Nano-$CaCO_3$
Waste management
Environmental pollution
Compressive strength
Flexural strength

Citation: Kumar A, Singh SK, Mishra A, Srivastava A (2026). Effect of polyethylene terephthalate granules on nano-$CaCO_3$-blended concrete. *Challenge Journal of Concrete Research Letters*, 17(1), 1–12.

1. Introduction

The cement industry is responsible for approximately 8–10% of all human-generated CO_2 emissions worldwide. With production projected to increase from around 4 billion metric tons today to more than 6 billion by 2050, this will further contribute to atmospheric CO_2 levels (Andrew 2018; Srivastava et al. 2025). In response, global initiatives are focusing on reducing the sector's environmental impact while still meeting rising demand. The cement technology roadmap presents key strategies for enhancing sustainability, including adopting energy-efficient processes, utilizing alternative fuels, reducing clinker content, and fostering technological innovation (Camiletti et al. 2013).

Among these approaches, clinker substitution stands out as a widely used and economical option. This technique involves partially replacing cement with supplementary cementitious materials such as fly ash, ground granulated blast furnace slag, silica fume, and limestone powder. Recently, nanotechnology has become increasingly popular, with nanomaterials being used as partial replacements for cement clinker. These nanoparticles modify the hydrated paste at the nanoscale, leading to notable improvements in compressive and flexural strength, as well as overall performance and durability (Srivastava et al. 2025; Cao et al. 2019). Research has demonstrated that adding nanoparticles including nano-SiO_2, nano-TiO_2, nano-$CaCO_3$, nano-Fe_2O_3, nano-ZrO_2, nano-Al_2O_3, and nano-graphene (as well as carbon nano-

* *Corresponding author.* E-mail address: kumarawadhesh0011@gmail.com (A. Srivastava)
ISSN: 2548-0928 / DOI: https://doi.org/10.20528/cjcrl.2026.01.001

tubes and carbon nanofibers to cementitious composites can significantly enhance their performance and longevity (d'Amora et al. 2020; Supit et al. 2014).

However, the high cost of many of these nanomaterials limits their widespread use in the cement industry. In comparison, nano-$CaCO_3$ is relatively more affordable and has been shown to potentially be produced at cement plants using waste CO_2 from cement production (Daniyal et al. 2019; Hashim et al. 2018).

In recent years, plastic production has steadily risen due to its widespread use in daily life. However, plastic waste is non-biodegradable and chemically hazardous, causing significant environmental harm. The United Nations Environment Program reports that global annual plastic production exceeds 400 million tonnes, with around 87% (or 350 million tonnes) becoming waste. As of 2015, the plastic packaging industry was generating approximately 141 million tonnes of single-use plastics annually, accounting for 47% of all plastic waste (Saikia et al. 2014). China emerged as the largest global producer of plastic packaging waste, contributing 40 million tonnes. Meanwhile, the United States had the highest per capita production of plastic packaging waste, totaling 45 million tonnes (Bamigboye et al. 2021).

Plastics come in two main types: thermoplastics and thermosetting plastics. Thermoplastics can be melted and recycled multiple times within the industry. Some common examples of thermoplastics include high-density polyethylene, low-density polyethylene, polyethylene terephthalate (PET), polyethylene, polystyrene, polypropylene, polyamide, polyoxymethylene, and polytetrafluoroethylene. In contrast, thermosetting plastics cannot be melted due to their strong molecular bonds and crosslinked structure, which makes them resistant to melting. Examples of thermosetting plastics are melamine, silicone, epoxy resin, phenolic, unsaturated polyester, and polyurethane. Currently, these plastic wastes are either incinerated or buried, both of which are expensive and environmentally damaging. Reusing thermosetting plastic waste could help reduce both pollution and waste management costs.

Among thermoplastics, PET is the most commonly used polyester. Frigione (2010) conducted research to evaluate the impact of replacing 5% of fine aggregates in concrete with unwashed PET particles by weight. The study assessed how this substitution influenced workability, compressive strength, and splitting tensile strength. Both the sand and PET particles used had sizes ranging from 300 μm to 2.36 mm. The results showed a slight decrease in compressive strength (less than 2%) and splitting tensile strength (between 1.6% and 2.4%) for the concrete with PET, but no significant change in workability. Almeshal et al. (2020) examined the effects of substituting sand with shredded PET waste (ranging from 0.075 to 4 mm) on concrete's workability, unit weight, and compressive strength, using replacement rates from 10% to 50% by volume. Their findings indicated that increasing the PET content significantly reduced workability, with slump values dropping from 90 mm for the control specimens to just 10 mm for those with 50% PET. This reduction in workability was attributed to PET's lower density compared to sand, which also adversely affected compressive strength. Concrete mixtures with 40% and 50% PET saw compressive strength reductions of 31% and 60%, respectively, compared to the control. Dawood et al. (2021) investigated concrete properties with shredded PET waste as a partial volumetric replacement of fine aggregates, ranging from 5% to 20%. Although both the fine aggregates and PET fibers were less than 4.75 mm in size, PET fibers predominantly ranged from 2.36 mm to 1.18 mm, with significant variation in gradation (0–4.47 mm). Their study found that workability decreased as PET content increased, with a notable 62.5% reduction for the 20% PET replacement compared to the control. This decrease was due to the larger surface area of PET particles. However, compressive strength improved with up to 15% PET replacement, peaking at a 7.5% increase for 12% PET, before declining with higher replacement levels (Choi et al. 2005).

Research on using PET waste as a partial replacement for concrete components (fine and coarse aggregates) has been conducted before, but results have varied based on the shape and size of the PET waste. While PET fibers have been commonly used, PET granules have not been extensively studied (Ismail and Al-Hashmi 2008). A recent study demonstrated that substituting 2% of cement with nano-$CaCO_3$ can lead to a 69% reduction in CO_2 emissions from cement production (Batuecas et al. 2021). Specifically, the CO_2 emissions decreased from 0.96 kg CO_2 eq./kg of cement to 0.3 kg CO_2 eq./kg. This reduction illustrates that nano-$CaCO_3$, even at lower replacement levels compared to fly ash, offers significant economic and environmental advantages (Aslani et al. 2021; Limami et al. 2020; Moghadam et al. 2009).

This research study investigates the impact of partial substitution of Polyethylene terephthalate (PET) with fine aggregate and nano calcium carbonate ($CaCO_3$) particles with cement in M40 grade concrete respectively. Important physical properties, were assessed alongside the microstructural observations. The cement is replaced by $CaCO_3$ with 0%, 2%, 3%, 4%, and 5%, while the fine aggregate is replaced by 10 % PET in all possible variations. This paper also examines the technical feasibility of incorporating nano-$CaCO_3$ in cement.

2. Materials and Method

2.1. Materials

In this study, the binder materials included only Ordinary Portland Cement (OPC) 43-grade in the control mixture, while the experimental mixtures used was OPC combined with nano-$CaCO_3$ particles. The nano-$CaCO_3$ particles employed had sizes ranging from 15 to 40 nm and contained 98% $CaCO_3$ shown in Fig. 1(a) (Siddique et al. 2008). The property of PET granules was shown in Table 1 and Fig. 1(b). A superplasticizer, commercially known as Fosroc (Complast SP40 G8 QCDA820), was used to enhance workability. Coarse aggregates with a maximum particle size of 20 mm and a specific gravity of 2.55 were utilized. Natural sand, with a specific gravity of 2.71, served as the fine aggregate. Tap water was used for mixing. The experimental test results of cement shown in Table 2.

Table 1. Characteristics of PET used in the experimental work.

Grade	Density	Manufacturer	Granule size	Source	Pre-treatment
B52A003	0.954 g/cm^3	Gail India G-Lex	≤ 4.75 mm	Post-consumer water bottles	Washed to remove impurities; air-dried; no chemical pre-treatment.

Table 2. Test results of OPC (43-grade) cement.

S. no	Properties	Test result
1	Specific gravity	3.04
2	Standard consistency	27%
3	Initial setting time	42 minutes
4	Final setting time	349 minutes

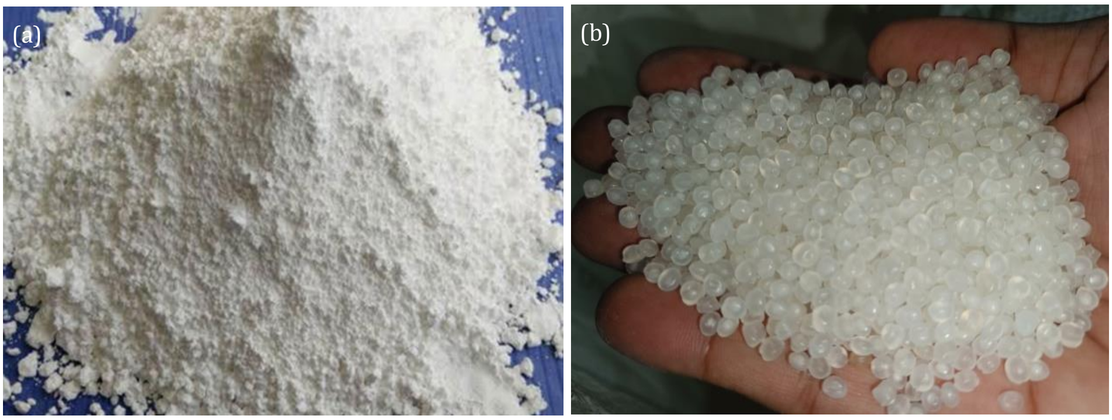

Fig. 1. (a) Nano-CaCO3; (b) PET granules.

2.2. Concrete mixes

Table 3 provides details on the mixing ratios for concrete mixes with varying amounts of nano-$CaCO_3$ as a replacement for cement. In the mix notation, “0NC10PP” indicates 0% nano-$CaCO_3$ replacement and 10% PET(PP) replacement. Concrete mixtures were prepared using different percentages of nano-$CaCO_3$ (0%, 2%, 3%, 4%, and 5%) relative to the dry cement weight, simultaneously PET was added at 10% of the fine aggregate weight for all different ratios. Small quantities of superplasticizer were incorporated into the mixtures to enhance the performance of the nano-particles (Limami et al. 2020).

Table 3. Mix design for the different concrete mix considered.

Sr. no	Concrete mix	Cement, kg/m^3	Fine aggregate, kg/m^3	Coarse aggregate, kg/m^3	Water cement ratio	Water, kg/m^3	Nano-$CaCO_3$, kg/m^3	PP granules, kg/m^3	Super plasticizer, l/m^3
1	0NC0PP	411.22	681.66	1191.75	0.36	143	0	0	1.85
2	0NC10PP	411.22	613.49	1191.75	0.36	143	0	68.17	1.85
3	2NC10PP	403.00	613.49	1191.75	0.36	143	8.22	68.17	1.85
4	3NC10PP	398.89	613.49	1191.75	0.36	143	12.33	68.17	1.85
5	4NC10PP	394.78	613.49	1191.75	0.36	143	16.44	68.17	1.85
6	5NC10PP	390.66	613.49	1191.75	0.36	143	20.56	68.17	1.85

2.3. Specimen casting and curing

To make the concrete mixes cement, coarse and fine aggregates with PET were combined in a rotary mixer. The aggregates used were in a saturated surface dry (SSD) condition. After mixing these ingredients, cement, nano-$CaCO_3$, water, and superplasticizer were added and mixed thoroughly. A portion of the fresh mixture was then tested for slump. After the slump test, the remaining mixture was kept in the mixer and poured into oiled molds. The molds were left to set for 24 hours as shown in Fig. 2. After this, the samples were removed from the molds and cured traditionally by immersing them in water for 7, 14, and 28 days (Siddique et al. 2008).

Fig. 2. Fresh concrete cube samples.

2.4. Specimen testing

First of all, compressive strength tests were performed on cubic samples with dimensions of 150×150×150 mm, while splitting tensile strength was tested using cylindrical samples of 100×200 mm. Flexural strength was assessed with beams measuring 150×150×700 mm. After conducting these tests on concrete samples that had cured for 28 days, some fragments were collected from the fractured surfaces. These fragments were then subjected to SEM and XRD analyses for detailed microstructural examination.

3. Results and Discussion

3.1. Workability

The control concrete mix recorded a slump value of 110mm as in Fig. 3. The rounded and relatively smooth PET granules facilitated the dispersion of fine aggregates in the mixture, despite the low water-to-cement ratio. Nano-CaCO3, being a natural material with finer particles than cement, enhances particle packing in concrete and acts as a spacer. Consequently, concrete mixtures with nano-$CaCO_3$ replacement exhibited a higher slump, improving workability. Concrete mixes with PET replacements showed a slump comparable to that of the control mix (Rahmani et al. 2013; Azhdarpour et al. 2016).

3.2. Density

The concrete density decreased with the addition of PET. For concrete with a 10% PET replacement, the density was 2405 kg/m^3, which is fairly close to the control sample's density of 2465 kg/m^3. Nano-$CaCO_3$ had minimal impact on the density, yielding similar results to those with PET. These results align with findings from other studies (Rahmani et al. 2013).

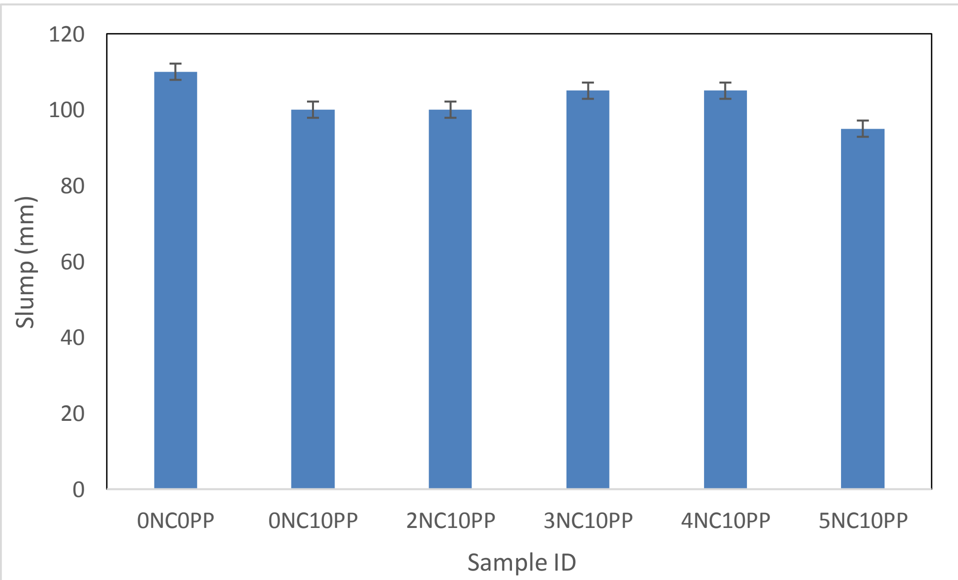

Fig. 3. Workability of the fresh concrete.

3.3. Compressive strength

The compressive strength of concrete increased by 4% with 10% PET granules, compared to the standard mix. However, adding 2% $CaCO_3$ and 10% PET granules achieved the target strength. The compressive strength of concrete dropped noticeably with higher $CaCO_3$ replacement ratios (Pezzi et al. 2006; Asha et al. 2015; Marangu et al. 2019). Differences in previous research results can be attributed to variations in the grading, shape, and size of PET particles, as well as the water-to-cement ratio used. The way PET granules affect the failure modes of concrete is related to their shape and flexibility.

When the concrete reaches its maximum load, the internal stresses shift from shear to tensile stress. Concrete with PET granules tends to maintain its shape after peak load, reducing the likelihood of collapse, whereas the standard concrete tends to be more brittle and fails through shear. This difference is likely due to the flexibility of PET granules compared to sand (Rahmani et al. 2013; Choi et al. 2005; Abu-Saleem et al. 2021). $CaCO_3$ interacts with the C_3A phase of cement to form carboalumination, which partially replaces ettringite. As a result, OPC concrete typically shows higher compressive strength than concrete with $CaCO_3$ at 28 days shown in Fig. 4, when the concrete has fully matured. Because nano-$CaCO_3$ is less reactive than cement, replacing cement with nano-$CaCO_3$ can lead to a decrease in compressive strength, especially over the long term, as there is minimal reaction between nano-$CaCO_3$ and cement hydrates (Rahmani et al. 2013; Choi et al. 2005).

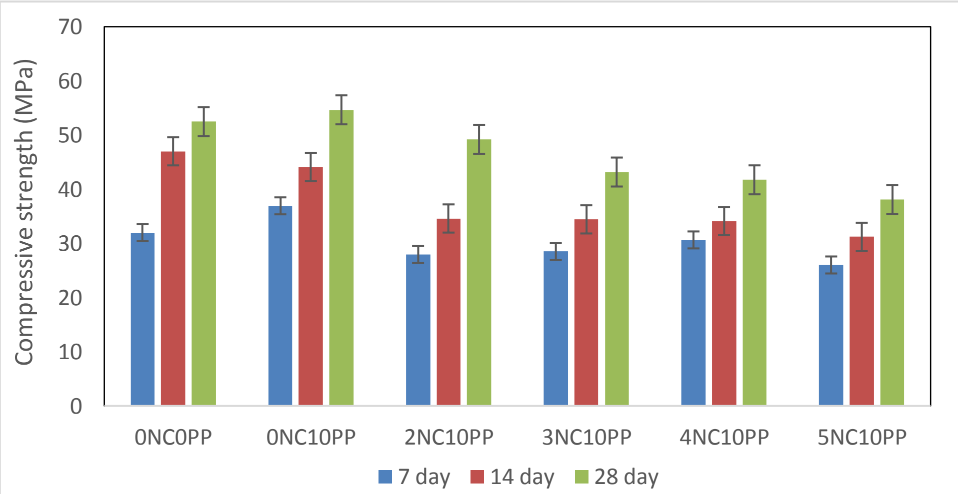

Fig. 4. Compressive strength test results of different mixes at 7, 14 and 28 days.

3.4. Tensile strength

The tensile strength dropped by 8% for the sample with 10% of PET and 0% of $CaCO_3$ compared to regular concrete as shown in Fig. 5. When more $CaCO_3$ was added, the performance worsened further. For instance, the sample with a 5% replacement rate saw a 14.15% decrease in tensile strength compared to the standard concrete. This happens because PET granules, when used in small amounts, helps in bonding the aggregates and cement better due to their flexibility and in even distribution (Fig. 6). However, once the concrete reaches its maximum strength, the PET granules tend to pull away from the cement, leading to reduced tensile strength (Pezzi et al. 2006, Asha et al. 2015).

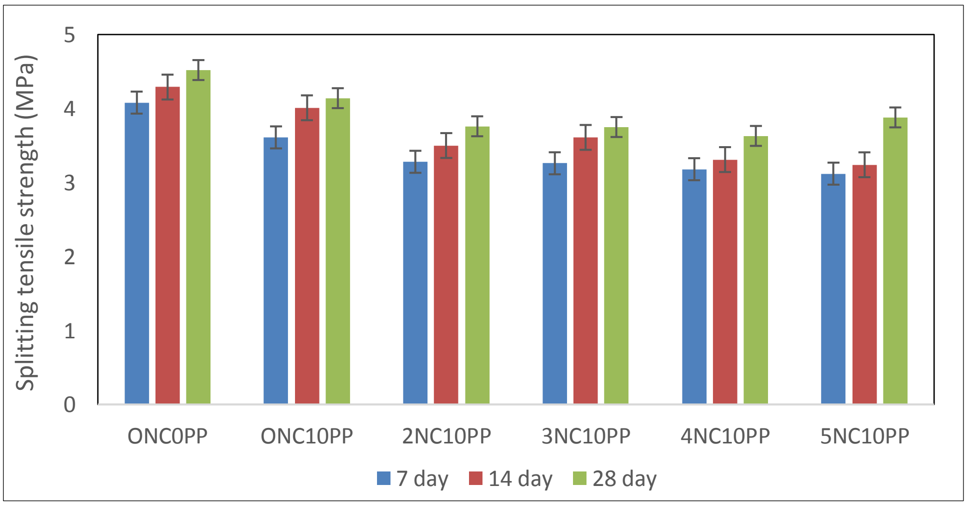

Fig. 5. Splitting tensile strength test results of different mixes at 7, 14 and 28 days.

Fig. 6. Splitting tensile strength test of cylindrical specimens.

3.5. Flexural strength

Test results in Fig. 7 show that the specimen containing 2% $CaCO_3$ and 10% PET reached the highest flexural strength of 3.23 MPa, which was a reduction of 2.71% compared to the reference concrete. Although the addition of $CaCO_3$ led to a decrease in flexural performance as its quantity increased, flexural strength remained relatively effective (Aslani et al. 2021). Fig. 8 denoted the fractured beam specimen during flexural test as per Indian standard.

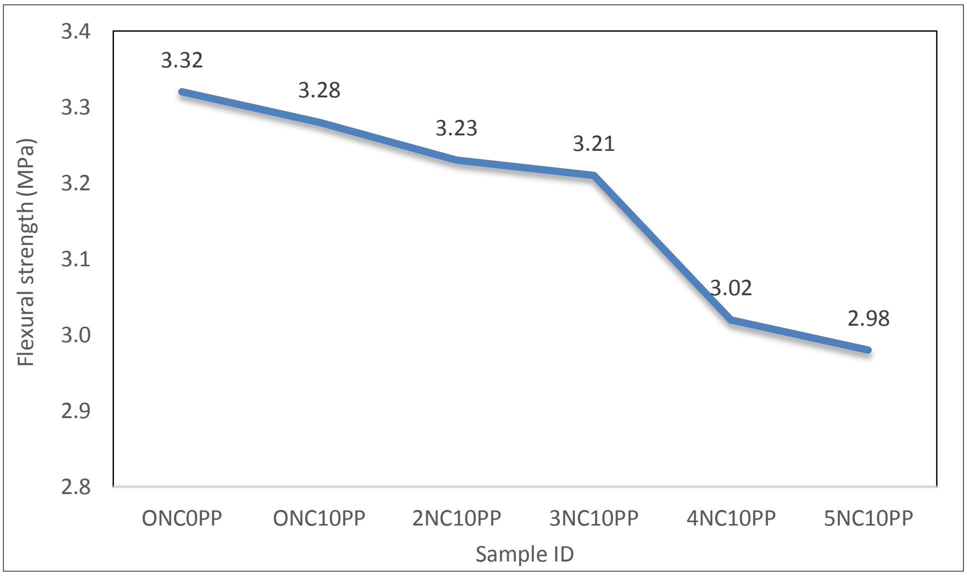

Fig. 7. Flexural strength test results at 28 days.

Fig. 8. Beam specimen after the flexural strength test.

3.6. Scanning electron microscopic (SEM) analysis

Fig. 9 shows the SEM micrographs of the 02NC10PP specimen, while Fig. 10 presents the corresponding EDS analysis used to identify its elemental composition.

Elemental composition:

- Oxygen (O): The high percentage of oxygen is expected in concrete due to the presence of various oxides and hydrated compounds such as calcium silicate hydrate (C-S-H), which is a major component of the cement matrix shown in Fig. 10.
- Aluminum (Al): Aluminum is present likely due to the aluminosilicate compounds found in the cementitious materials. Al might be a part of phases like calcium aluminate hydrates or fly ash additives if used.
- Silicon (Si): Silicon is a major component in concrete due to the presence of silicon dioxide (SiO_2) in sand and other aggregates. It is also a primary component of the C-S-H gel formed during the hydration of cement.
- Potassium (K): Potassium could be from the raw materials used in cement. It can also be from K-feldspar in the aggregates.
- Calcium (Ca): Calcium is a key element in concrete, primarily from the calcium carbonate ($CaCO_3$) nanoparticles added, as well as from calcium silicates and calcium hydroxide formed during hydration of cement.
- Platinum (Pt): Platinum is not a common component of concrete and its presence here is most likely from a coating applied to the sample for SEM analysis to make it conductive. This coating improves the quality of the SEM images.

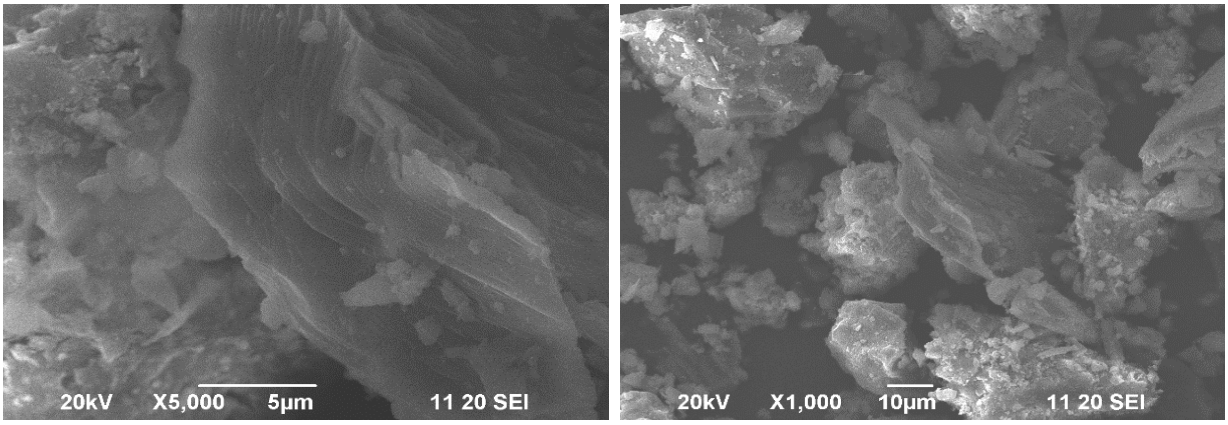

Fig. 9. SEM images of 02NC10PP.

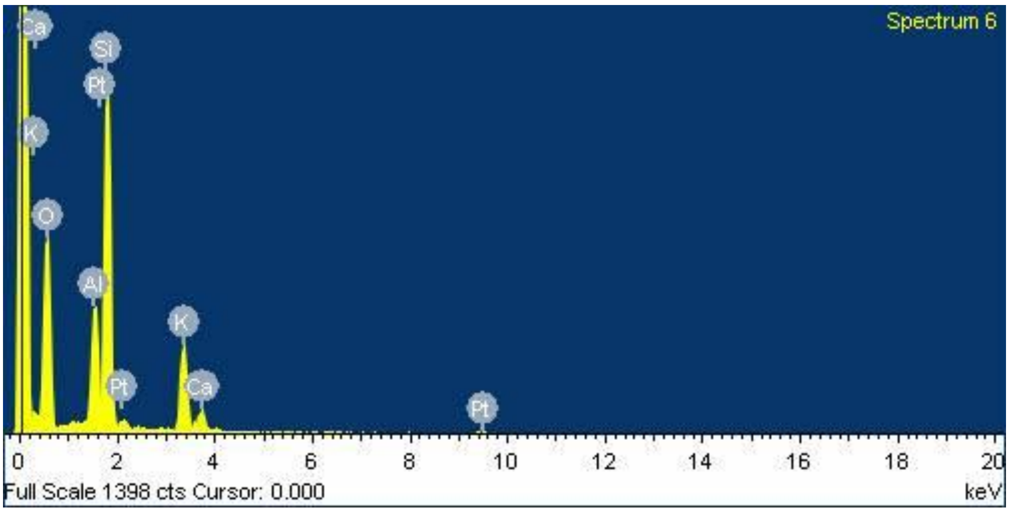

Fig. 10. EDS image of 02NC10PP.

Implications and observations:

- Nano-$CaCO_3$ and Concrete Composition: The presence of calcium (Ca) at 1.56% by weight suggests that the nano-$CaCO_3$ is dispersed throughout the sample. Although it is a small percentage, nano-$CaCO_3$ can significantly influence the microstructure and mechanical properties of concrete by acting as a filler and nucleation site for hydration products.
- Polyethylene terephthalate (PET) Granules: The analysis does not directly detect PET because it is a car-bon-based polymer and typically does not produce characteristic X-rays detectable by EDS. The influence of PET granules would be more evident in mechanical property tests and microstructural analysis rather than in elemental composition data from EDS.
- Concrete Matrix: The high content of oxygen, silicon, and aluminum suggests the formation of typical cementitious compounds such as C-S-H, ettringite, and other hydration products shown in Fig. 9. The pres-

ence of potassium and other elements aligns with typical raw materials and potential additives.
- Platinum Coating: The presence of 2% platinum is due to the conductive coating applied to the sample. This is a standard preparation step for SEM analysis to prevent charging and to improve image resolution.

The SEM-EDS analysis of the concrete sample containing 2% nano-$CaCO_3$ and 10% PET granules shows a typical composition with major elements expected in a cementitious matrix. The nano-$CaCO_3$ is present as indicated by the calcium content, while the PET granules, being non-metallic and non-oxide, are not directly detectable by EDS but contribute to the mechanical and durability properties of the concrete. The analysis confirms the expected distribution of elements in a concrete matrix modified with nano-$CaCO_3$ and PET granules represents in Table 4 (Aslani et al. 2021; Azhdarpour et al. 2016).

Table 4. EDS elemental composition of 02NC10PP.

Element	Weight, %	Atomic, %
O	58.67	73.45
Al	7.33	5.44
Si	22.54	16.08
K	7.90	4.05
Ca	1.56	0.78
Pt	2.00	0.21
Totals	100.00	–

Fig. 11 shows the SEM micrographs of the 05NC10PP specimen, while Fig. 12 presents the corresponding EDS analysis used to identify its elemental composition.

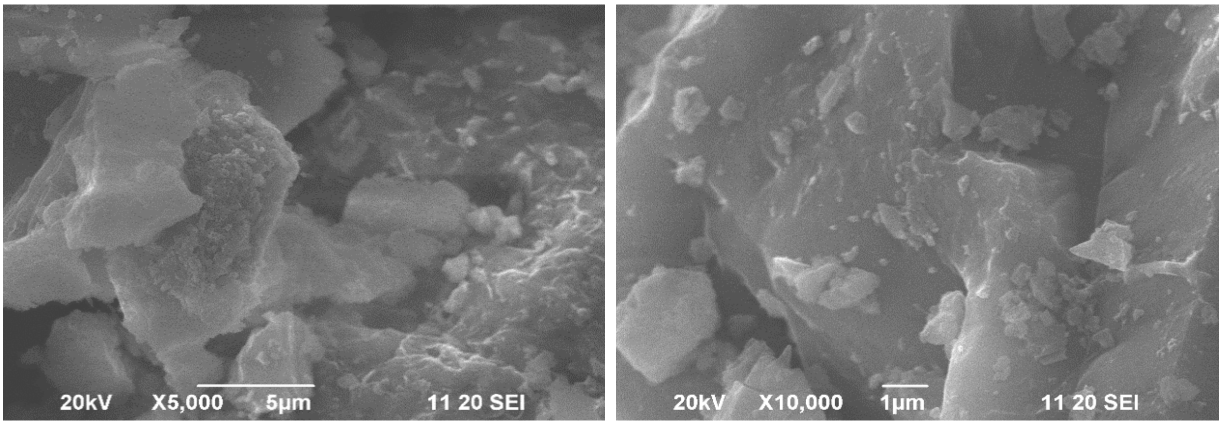

Fig. 11. SEM images of 05NC10PP.

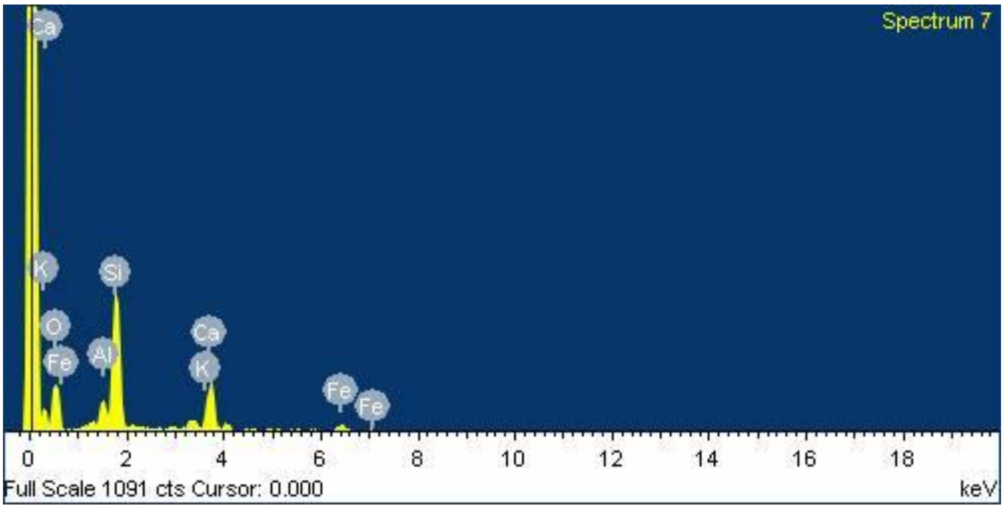

Fig. 12. EDS image 05NC10PP.

Elemental composition:
- Oxygen (O): The high percentage of oxygen is typical in concrete, reflecting the presence of various oxides and hydrated compounds. This includes calcium silicate hydrate (C-S-H), calcium hydroxide, and other hydration products.
- Aluminum (Al): Aluminum is present due to the aluminosilicate compounds in the cementitious materials. It may come from the raw materials or additives like fly ash.
- Silicon (Si): Silicon is a significant component in concrete, originating from silicon dioxide (SiO_2) in sand, aggregates, and the C-S-H gel formed during the hydration of cement.
- Potassium (K): Potassium can come from raw materials used in cement, pozzolans, or fly ash additives. It

might also be present in K-feldspar from aggregates Fig. 12.

- Calcium (Ca): The relatively high percentage of calcium indicates the presence of calcium compounds, including the 3% nano-$CaCO_3$ added. Calcium is essential in forming calcium silicate hydrates and other cement hydration products.
- Iron (Fe): Iron might be present in small amounts from raw materials used in cement production, or it could be a trace element from aggregates or additives. Iron oxides can also contribute to the color and durability of concrete.

Implications and observations:

- Nano-$CaCO_3$ and Concrete Composition: The presence of calcium at 12.59% by weight suggests a significant influence of nano-$CaCO_3$ on the overall composition. The increased calcium content compared to the previous sample with 1% nano-$CaCO_3$ indicates the higher incorporation of these nanoparticles, enhancing the concrete's microstructure and potentially improving its mechanical properties.
- PET Granules: Similar to the previous analysis, the PET granules, being carbon-based, are not directly detectable by EDS. Their impact on the concrete would be more evident in its mechanical properties and microstructure, providing improved toughness and crack resistance.
- Concrete Matrix: The high content of oxygen, silicon, and aluminum suggests the formation of typical cementitious compounds, such as C-S-H, ettringite, and other hydration products. The presence of potassium and iron aligns with typical raw materials and potential additives Fig. 12.
- Oxygen and Silicon: Both samples have high oxygen and silicon contents, typical of cementitious materials.
- Aluminum: The aluminum content is slightly lower in the 5% nano-$CaCO_3$ sample.
- Calcium: The calcium content is significantly higher in the 5% nano-$CaCO_3$ sample, reflecting the increased addition of nano-$CaCO_3$.
- Iron: The new sample has a measurable amount of iron, which was not present in the previous analysis, indicating possible variations in the raw materials or additives used.

The SEM-EDS analysis of the concrete sample with 5% nano-$CaCO_3$ and 10% PET granules shows a typical composition with significant calcium content due to the increased nano-$CaCO_3$ addition shown in Fig. 11. The elemental composition suggests the formation of standard cementitious phases, with the added nano-$CaCO_3$ likely improving the microstructure and mechanical properties of the concrete as shown in Table 5. The PET granules, while not detectable by EDS, contribute to enhanced toughness and crack resistance. The presence of iron in this sample indicates some variation in raw materials or additives compared to the previous sample (Marangu et al. 2019; Rahmani et al. 2013; Abu-Saleem et al. 2021).

Table 5. EDS elemental composition of 05NC10PP.

Element	Weight, %	Atomic, %
O	52.73	69.14
Al	4.10	3.19
Si	24.85	18.56
K	2.31	1.24
Ca	12.59	6.59
Fe	3.42	1.28
Totals	100.00	–

3.7. X-ray diffraction (XRD) analysis

As shown in Fig. 13, the XRD pattern of the 2NC10PP specimen indicates the presence of distinct crystalline phases within the concrete matrix. The intensity peaks represent the constructive interference of diffracted X-rays, while the 2θ values correspond to specific lattice planes of the crystalline constituents. The most prominent peaks can be associated with calcium carbonate, particularly those observed around 24° to 25° and 29° to 30°. In particular, the peak near 29.4° is characteristic of the (104) plane of calcite, confirming the presence of $CaCO_3$ in the specimen. In addition, the peaks detected at higher diffraction angles may be attributed to other crystalline phases present in the cementitious matrix, including hydration products and mineral constituents. The incorporation of nano-$CaCO_3$ may also act as a nucleation site, contributing to microstructural refinement and supporting the mechanical performance of the concrete.

Similarly, Fig. 14 shows the XRD pattern of the 5NC10PP specimen, which also exhibits several sharp peaks indicating well-defined crystalline phases. The most prominent peaks appear around 24.77°, 30.61°, and 50.07° 2θ, suggesting the presence of calcite and other crystalline compounds in the matrix. Moreover, several smaller peaks are distributed across the diffraction range, indicating minor phases that may be associated with cement hydration products such as calcium silicate hydrates and ettringite. The higher $CaCO_3$ content in this mixture may explain the stronger calcite-related reflections. Although PET-related phases are difficult to identify directly because of peak overlap and the polymeric nature of PET, the XRD pattern still confirms that the concrete contains the expected crystalline components of a modified cementitious composite.

4. Numerical Verification Through Software

The compressive strength data for concrete specimens 0NC0PP, 0NC10PP, 2NC10PP, 3NC10PP, 4NC10PP, and 5NC10PP were verified using ANSYS Workbench 2024 R2. The comparison between the experimental and numerical results is shown in Fig. 15. A standard-sized concrete cube with dimensions of 150 mm × 150 mm × 150 mm was modeled in ANSYS Workbench 2024 R2. To analyze the stress distribution of the concrete cube, the following procedure was adopted:

- First, a new static structural analysis system was created in the Workbench project. After that, the geometry was defined, and a cube with the specified dimensions was created.
- Material properties were assigned by selecting concrete and inputting the experimental density value.
- Other relevant material properties such as Young's modulus and Poisson's ratio were also assigned.
- The analysis then proceeded to the meshing stage by generating a suitable mesh for the cube. In this setup, boundary conditions were applied by fixing one face of the cube to simulate a fixed support.
- A load was then applied on the opposite face in the negative y-axis direction.
- After setting up the boundary conditions and loading, the model was solved.
- Once the solution was complete, the results were reviewed by plotting the equivalent (von Mises) stress distribution to understand the stress behavior within the concrete cube under the given loading conditions. Table 6 presents the comparison between the experimental and analytical data.

Table 6. Compressive strength at 28th day (MPa).

Concrete mix	Experiment	Numerical
0NC0PP	52.49	53.23
0NC10PP	54.675	55.12
2NC10PP	47.21	47.59
3NC10PP	43.17	43.75
4NC10PP	41.73	42.57
5NC10PP	38.11	39.14

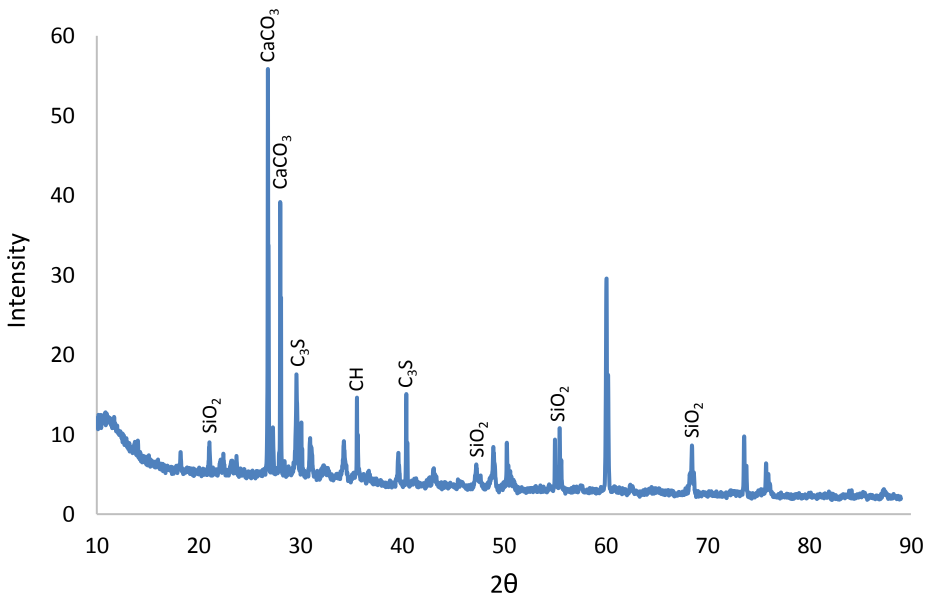

Fig. 13. XRD data of 2NC10PP.

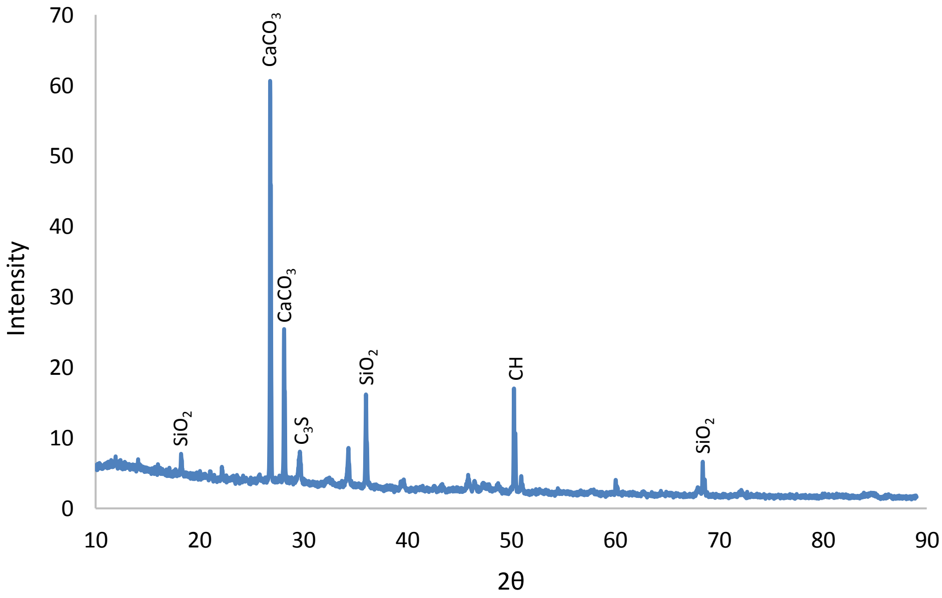

Fig. 14. XRD data of 5NC10PP.

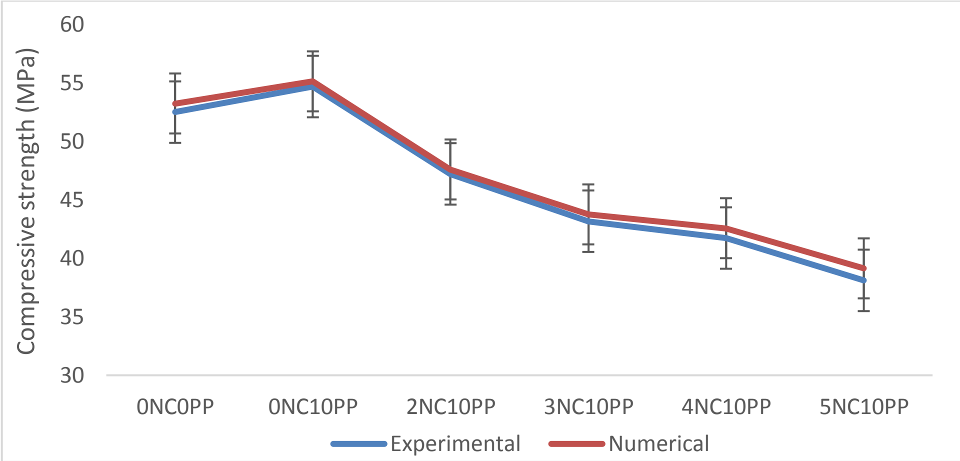

Fig. 15. Comparison of stresses for experimental and numerical approach.

5. Conclusions

This study examines how PET granules and nano-$CaCO_3$ affect the fresh, hardened, and microstructural properties of M40 concrete. PET granules were used to replace 10% of the fine aggregates, and nano-$CaCO_3$ was mixed with the cement on a volumetric basis. The PET granules were sized to closely match the river sand they replaced to reduce any effects from size differences. Based on the results, the following conclusions can be drawn:

- Adding up to 2% nano-$CaCO_3$ with PET granules did not affect the workability of the concrete mix. However, beyond this amount, the workability decreased with increasing nano-$CaCO_3$ content, although the reduction was minimal. Similarly, the density of the concrete decreased as more nano-$CaCO_3$ and PET granules were added, because PET is lighter than sand.
- Concrete with 10% PET granule content exceeded the target compressive strength for M40 concrete. The compressive strength of concrete increased by 4% with 10% PET granules compared to the standard mix. In contrast, concrete with 2% nano-$CaCO_3$ and 10% PET granule content achieved the target strength.
- The compressive strength of $CaCO_3$ concrete is slightly lower than that of standard concrete. This is due to $CaCO_3$ reacting with the C_3A phase of the cement to form carboaluminate, which partially replaces ettringite. Consequently, OPC concrete has a higher compressive strength at 28 days, when the concrete is fully cured. Since $CaCO_3$ is less reactive than cement, its replacement leads to a reduction in compressive strength, partly because $CaCO_3$ has minimal interaction with cement hydrates and does not provide the same long-term pozzolanic activity.
- The tensile strength declined with increasing nano-$CaCO_3$ content, although the change was relatively minor.
- The inclusion of PET granules up to a 10% replacement ratio positively impacted both flexural strength and toughness, with the greatest improvements observed in specimens containing 10% PET granules. However, when nano-$CaCO_3$ was added alongside PET, both flexural strength and toughness decreased.
- SEM images revealed a uniform distribution of $CaCO_3$ in the concrete mix, while the PET granules, being non-metallic and non-oxide, are not directly detectable by EDS but contribute to the mechanical and durability properties of the concrete.
- The XRD pattern provides a fingerprint of the crystalline components present in the concrete sample. By analyzing the peaks and their positions, one can deduce the presence and concentration of specific phases, such as calcium carbonate from the nano-$CaCO_3$ and other crystalline constituents of the concrete. The incorporation of nano-$CaCO_3$ and PET granules is aimed at improving the mechanical and durability properties of the concrete, which is reflected in the XRD pattern through the identified phases and their intensities.
- The results of this study, in terms of compressive strength, tensile strength, and flexural strength, were notably higher compared to findings reported in the literature, especially for concrete mixtures containing 10% PET granules.
- The compressive strength of concrete containing nano-$CaCO_3$ with PET granules was found to be nearly similar to the results predicted by ANSYS.

Acknowledgements

The authors would like to thank Institute of Engineering and Technology, Lucknow, India for the support regarding the experimental research.

Funding

The authors received no financial support for the research, authorship, and/or publication of this manuscript.

Conflict of Interest

The authors declare no potential conflicts of interest with respect to the research, authorship, and/or publication of this manuscript.

Data Availability

The datasets generated and/or analyzed during the current study are not publicly available but are available from the corresponding author upon reasonable request.

AI Assistance

No AI-based tools were used in the preparation of this manuscript.

Author Contributions

All authors made substantial contributions to the conception and design of the study, acquisition of data, analysis and interpretation of data; drafted or critically revised the manuscript for important intellectual content; and approved the final version to be published.

REFERENCES

Abu-Saleem M, Zhuge Y, Hassanli R, Ellis M, Rahman MM, Levett P (2021). Microwave radiation treatment to improve the strength of recycled plastic aggregate concrete. *Case Studies in Construction Materials*, 15, e00728.

Almeshal I, Tayeh B A, Alyousef R, Alabduljabbar H, Mohamed AM (2020). Eco-friendly concrete containing recycled plastic as partial replacement for sand. *Journal of Materials Research and Technology*, 9(3), 4631-4643.

Andrew RM (2018). Global CO_2 emissions from cement production. *Earth System Science Data*, 10, 195–217.

Asha S, Resmi PR (2015). Experimental research on concrete with straight and crimped waste plastic fibres. *International Journal of Engineering Sciences & Emerging Technologies*, 8(2), 55-71.

Aslani H, Pashmtab P, Shaghaghi A, Mohammadpoorasl A, Taghipour H, Zarei M (2021). Tendencies towards bottled drinking water consumption: Challenges ahead of polyethylene terephthalate (PET) *waste management*. *Health Promotion Perspectives*, 11(1), 60-68.

Azhdarpour AM, Nikoudel, MR, Taheri M (2016). The effect of using polyethylene terephthalate particles on physical and strength-related properties of concrete; a laboratory evaluation. *Construction and Building Materials*, 109, 55-62.

Bamigboye GO, Tarverdi K, Umoren A, Bassey DE, Okorie U, Adediran J (2021). Evaluation of eco-friendly concrete having waste PET as fine aggregates. *Cleaner Materials*, 2, 100026.

Batuecas E, Liendo F, Tommasi T, Bensaid S, Deorsola FA, Fino D (2021). Recycling CO_2 from flue gas for $CaCO_3$ nanoparticles production as cement filler: A life cycle assessment. *Journal of CO_2 Utilization*, 45, 101446.

Camiletti J, Soliman, AM, Nehdi ML (2013). Effects of nano- and micro-limestone addition on early-age properties of ultra-high-performance concrete. *Materials and Structures/Materiaux et Constructions*, 46, 881–898.

Cao M, Ming X, He K, Li L, Shen S (2019). Effect of macro-, micro-and nano-calcium carbonate on properties of cementitious composites—A review. *Materials*, 12(5), 781.

Choi YW, Moon DJ, Chung JS, Cho SK (2005). Effects of waste PET bottles aggregate on the properties of concrete. *Cement and Concrete Research*, 35(4), 776-781.

d'Amora M, Liendo F, Deorsola FA, Bensaid S, Giordani S (2020). Toxicological profile of calcium carbonate nanoparticles for industrial applications. *Colloids and Surfaces B: Biointerfaces*, 190, 110947.

Daniyal M, Akhtar S, Azam A (2019). Effect of nano-TiO2 on the properties of cementitious composites under different exposure environments. *Journal of Materials Research and Technology*, 8, 6158–6172.

Dawood AO, Hayder AK, Falih RS (2021). Physical and mechanical properties of concrete containing PET wastes as a partial replacement for fine aggregates. *Case Studies in Construction Materials*, 14, e00482.

Frigione M (2010). Recycling of PET bottles as fine aggregate in concrete. *Waste Management*, 30(6), 1101-1106.

Hashim AM, Nhabah HT (2018). Influence of $CACO_3$ with nanoparticles on the mechanical characteristics and concrete microstructure. *International Journal of Civil Engineering and Technology*, 9, 799–808.

Ismail ZZ, Al-Hashmi EA (2008). Use of waste plastic in concrete mixture as aggregate replacement. *Waste Management*, 28(11), 2041-2047.

Limami H, Manssouri I, Cherkaoui K, Saadaoui M, Khaldoun A (2020). Thermal performance of unfired lightweight clay bricks with HDPE & PET waste plastics additives. *Journal of Building Engineering,* 30, 101251.

Marangu JM, Thiong'o JK, Wachira JM (2019). Review of carbonation resistance in hydrated cement based materials. *Journal of Chemistry*, 2019(1), 8489671.

Moghadam MA, Mokhtarani N, Mokhtarani B (2009). Municipal solid waste management in Rasht City, Iran. *Waste Management*, 29(1), 485-489.

Pezzi L, De Luca PA, Vuono D, Chiappetta F, Nastro A (2006). Concrete products with waste's plastic material (bottle, glass, plate). In: *Materials Science Forum*, 514-516, 1753-0.

Rahmani E, Dehestani M, Beygi MHA, Allahyari H, Nikbin IM (2013). On the mechanical properties of concrete containing waste PET particles. *Construction and Building Materials*, 47, 1302-1308.

Saikia N, De Brito, J (2014). Mechanical properties and abrasion behaviour of concrete containing shredded PET bottle waste as a partial substitution of natural aggregate. *Construction and Building Materials*, 52, 236-244.

Siddique R, Khatib J, Kaur I (2008). Use of recycled plastic in concrete: A review. *Waste Management*, 28(10), 1835-1852.

Srivastava A, Mishra A, Singh S (2025). Mechanical and durability study of nano-SiO_2 and nano-TiO_2 on fiber reinforced concrete. *Challenge Journal of Concrete Research Letters*, 16(1), 33-39.

Srivastava A, Mishra A, Singh, SK (2025). Effect of nano TiO_2 and reinforcement of polypropylene fiber in standard concrete: an experimental and numerical approach. *Canadian Journal of Civil Engineering*, 52(5), 929-945.

Supit SWM, Shaikh FUA (2014). Effect of Nano-$CaCO_3$ on compressive strength development of high volume fly ash mortars and concretes. *Journal of Advanced Concrete Technology*, 12, 178–186.